

Special Issue Research Articles

Reactive Oxygen Species Explicit Dosimetry for Photofrin-mediated Pleural Photodynamic Therapy[†]

Yi Hong Ong^{1,2} , Andreaa Dimofte¹, Michele M. Kim¹, Jarod C. Finlay¹, Tianqi Sheng¹, Sunil Singhal³, Keith A. Cengel¹, Arjun G. Yodh², Theresa M. Busch¹  and Timothy C. Zhu^{*1} 

¹Department of Radiation Oncology, University of Pennsylvania, Philadelphia, PA

²Department of Physics and Astronomy, University of Pennsylvania, Philadelphia, PA

³Division of Thoracic Surgery, Department of Surgery, University of Pennsylvania, Philadelphia, PA

Received 6 September 2019, accepted 18 October 2019, DOI: 10.1111/php.13176

ABSTRACT

Explicit dosimetry of treatment light fluence and implicit dosimetry of photosensitizer photobleaching are commonly used methods to guide dose delivery during clinical PDT. Tissue oxygen, however, is not routinely monitored intraoperatively even though it is one of the three major components of treatment. Quantitative information about *in vivo* tissue oxygenation during PDT is desirable, because it enables reactive oxygen species explicit dosimetry (ROSED) for prediction of treatment outcome based on PDT-induced changes in tumor oxygen level. Here, we demonstrate ROSED in a clinical setting, Photofrin-mediated pleural photodynamic therapy, by utilizing tumor blood flow information measured by diffuse correlation spectroscopy (DCS). A DCS contact probe was sutured to the pleural cavity wall after surgical resection of pleural mesothelioma tumor to monitor tissue blood flow (blood flow index) during intraoperative PDT treatment. Isotropic detectors were used to measure treatment light fluence and photosensitizer concentration. Blood-flow-derived tumor oxygen concentration, estimated by applying a preclinically determined conversion factor of $1.5 \times 10^9 \mu\text{Ms cm}^{-2}$ to the blood flow index, was used in the ROSED model to calculate the total reacted reactive oxygen species [ROS]rx. Seven patients and 12 different pleural sites were assessed and large inter- and inpatient heterogeneities in [ROS]rx were observed although an identical light dose of 60 J cm^{-2} was prescribed to all patients.

INTRODUCTION

Light, photosensitizer and tissue oxygen are the three most important factors required by photodynamic therapy (PDT) to produce reactive oxygen species (ROS) that kill tumor cells directly, damage tumor vasculature and stimulate the body's immune response (1–3). In clinical practice, PDT is generally prescribed as a drug dose (mg of photosensitizer per kg of body weight) and a treatment light fluence (J cm^{-2}), along with a

drug-light interval and a light fluence rate (mW cm^{-2}). Dosimetry of light fluence is routinely performed to guide PDT delivery, but the delivered light doses are limited in terms of their accuracy for predicting treatment outcome because they do not account for the variation in tissue optical properties, the pharmacokinetics and photobleaching of photosensitizer and tumor oxygenation during PDT (4–6). Compared to the light fluence and photosensitizer photobleaching ratio, PDT dose defined as the absorbed light dose by the photosensitizer during PDT has been shown to be a better dosimetric quantity for prediction of treatment outcome as long as the oxygen supply is sufficient (4–6). However, this PDT dose metric is less effective when tissue is deprived of oxygen. Since both photochemical consumption of oxygen and microvascular shutdown can lead to tissue hypoxia during PDT, ROS produced via the interactions of all three PDT inputs is the best dose metric for prediction of treatment outcomes. ROS effectively accounts for temporal changes in the light, photosensitizer and tissue oxygen during PDT (5–12). Direct measurement of ROS, however, is very challenging in clinical settings due to the extremely weak signal and the short lifetime of ROS (13–15).

Our work employs an approach based on an empirical macroscopic reactive oxygen species explicit dosimetry (ROSED) model that has been proposed to calculate the total amount of reacted reactive oxygen species ([ROS]rx). The model utilizes the light diffusion equation and the complete set of PDT kinetic equations which quantify dynamic interactions between the light, the photosensitizer concentration and the tissue oxygenation (16,17). Recent studies in mice models suggest that measurement of tissue oxygen is necessary to improve calculation of [ROS]rx, especially for Photofrin-mediated PDT, due to large heterogeneity in PDT-induced physiologic response (4,8,9). The ROSED model-calculated tissue oxygen ($^3\text{O}_2$) concentrations were found to be in good agreement with measured values for mice treated by BPD- and HPPH-mediated PDT, but the large mouse-to-mouse variations in the temporal changes of $[\text{}^3\text{O}_2]$ for Photofrin-mediated PDT were difficult to model mathematically using ROSED (8,9). Moreover, although there is a plethora of established techniques for *in vivo* tissue oxygen measurement, to the best of our knowledge, the Food and Drug Administration (FDA) has not approved an instrument which can be used to measure tissue oxygen noninvasively in patients during PDT.

*Corresponding author e-mail: timothy.zhu@penmedicine.upenn.edu (Timothy C. Zhu)

[†]This article is part of a Special Issue dedicated to Dr. Jarod C. Finlay.

© 2019 American Society for Photobiology

Here, we demonstrate the potential use of tumor blood flow to perform ROSED when tissue oxygen information is not available during clinical PDT. Blood flow can be measured noninvasively using an optical modality known as diffuse correlation spectroscopy (DCS). First, we investigated the relationship between tumor blood flow and tumor oxygen during Photofrin-mediated PDT of mice bearing radiation-induced fibrosarcoma (RIF) tumors. Based on the resulting preclinically determined blood flow to oxygen conversion factor, we performed ROSED for Photofrin-mediated photodynamic therapy of patients with malignant pleural mesothelioma. Explicit measurements of light fluence rate and fluorescence measurements of Photofrin concentration were performed using an isotropic detector. A custom DCS contact probe was sutured adjacent to the isotropic detector to measure blood flow of the pleural cavity wall concurrently during PDT delivery. Information about light fluence, Photofrin concentration and blood-flow-derived oxygen were then used in calculation of [ROS]rx. Different dose metrics, including light fluence, PDT dose and [ROS]rx were also compared and assessed for intra- and interpatient heterogeneity.

MATERIALS AND METHODS

Tumor model and PDT treatment conditions. We conducted a preclinical study using a murine model to investigate the relationship between the dynamics of tumor oxygen and blood flow during PDT. Female C3H mice (Charles River Laboratories, Kingston, NY) between 6 to 8 weeks of age were used in this study. Radiation-induced fibrosarcoma (RIF) tumors were propagated on the shoulders of mice by intradermal injection of 3×10^5 cells. The mice were fed with chlorophyll-free (alfalfa-free) rodent diet (Harlan Laboratories Inc., Indianapolis, Indiana, USA) for two weeks prior to treatment to eliminate the fluorescence signal from chlorophyll-breakdown products, which overlap with the emission spectrum of Photofrin fluorescence. Fluorescence measurements were taken every day after they were fed with the modified diet to evaluate and confirm the elimination of chlorophyll contamination on Photofrin fluorescence during PDT treatment. PDT was performed when tumors reached ~4–5 mm in diameter. The treatment area was depilated with Nair (Church & Dwight Co., Inc., Ewing, NJ, USA) and 5 mg kg⁻¹ Photofrin was injected via tail vein 24 h prior to measurements and light delivery. Tissue optical properties and Photofrin fluorescence spectra were obtained using a custom-made multifiber contact probe, as described elsewhere (18,19), before and after PDT. Tissue oxygenation and blood flow changes were monitored continuously during the delivery of PDT using oximeter and DCS as described below. At a 24-h drug–light interval, superficial irradiation of the tumor was performed with a 630-nm laser (Biolitec AG., A-1030, Vienna). A microlens fiber was coupled to the laser to irradiate the tumor uniformly. The details of the PDT treatment conditions are summarized in Table 2. Animals used in this study were under the care of the University of Pennsylvania Laboratory Animal Resources and the studies were approved by the University of Pennsylvania Institutional Animal Care and Use Committee.

Measurement of tumor tissue oxygenation during preclinical PDT. Tumor oxygen was monitored throughout the PDT treatment in mice using an optical oxygen partial pressure (pO₂) monitor (OxyLite Pro, Oxford Optronix, Oxford, UK), with a bare-fiber-type probe (NX-BF/O/E, Oxford Optronix, Oxford, UK). The tip of the probe was inserted into the tumor at approximately 1–2 mm depth from the treatment surface to measure the changes in tissue oxygen partial pressure within the tumor mass during PDT. ³O₂ concentration was then approximated by multiplying the measured pO₂ with ³O₂ solubility in tissue, which is 1.295 μM mmHg⁻¹ (20,21).

Diffuse correlation spectroscopy (DCS) for blood flow measurement. DCS is an optical spectroscopic technique that measures the rapid speckle intensity fluctuation induced by blood flow. Specifically, DCS derives blood flow information from the temporal intensity autocorrelation function of the detected multiply scattered light (22). DCS employs coherent near-infrared light that travels diffusively through tissue and scattered multiple times before emerging from tissue surface.

During each scattering event, the phase of the scattered light is altered. At the detector, multiple light fields that have traveled along different paths through the tissue, and thus have different phases, will interfere constructively and destructively and create a speckle pattern. Dynamic scatterings of the moving red blood cells cause the speckle pattern to change in time. As these temporal intensity fluctuations of the detected light are sensitive to the motions of red blood cells in the tissue microvasculature, the DCS signals provide a direct measure of blood flow. These temporal fluctuations can be quantified by computing the normalized intensity temporal autocorrelation function, $g_2(\tau) \equiv \langle I(t)I(t+\tau) \rangle / \langle I(t) \rangle^2$, at multiple delay-times, τ , where $I(t)$ is the intensity of the detected light at time t , and the angular brackets, $\langle \rangle$, represent time averages. Normalized electric field autocorrelation function, $g_1(\tau) = G_1(\tau)/G_1(\tau=0)$ is then derived from measurements of $g_2(\tau)$ via the Siegert relation (23): $g_2(\tau) = 1 + \beta|g_1(\tau)|^2$, where β is a constant determined primarily by the experimental collection optics. The electric field autocorrelation function, $G_1(\tau) \equiv \langle E^*(t)E(t+\tau) \rangle$ obeys a correlation diffusion equation in highly scattering media (24,25). Blood flow index (*BFI*) is obtained by fitting $g_1(\tau)$ to the analytical solution of the correlation diffusion equation in the semi-infinite geometry (26).

Measurement of blood flow during preclinical PDT. DCS, within a noncontact probe setup, was used to monitor blood flow changes in mice during PDT. A detailed description of the DCS instrument can be found in (22,27). Briefly, a continuous wave 785-nm laser with long coherence length (CrystalLaser Inc., Reno, NV) delivered light through a source fiber, and the diffuse reflected light was collected using two single-mode fibers located 0.3 cm laterally from the source fiber. These fibers were mounted on the imaging plane of a camera with sensor removed. A camera lens was used to focus the laser and to collect diffuse reflected light from the tumor at a fixed distance of 15 cm from the camera lens. This detected light has probed a “banana shaped” volume of tissue that span ~1/2 of the source detector separation (*i.e.* ~0.15 cm) below tissue surface (28,29). This setup permits noncontact measurements of blood flow during PDT without obstructing the treatment light. Two single photon counting avalanche photodiodes were used to detect the diffuse light in parallel. Notch filters at 630 nm and a 785 nm bandpass filter were used to prevent the ambient room light and the strong 630 nm treatment laser from saturating the detectors. Tissue blood flow measurements started 5 min before the beginning of PDT treatment and lasted until completion of PDT.

Clinical PDT treatment and PDT dose detection. The primary goal of this study is to demonstrate and perform explicit dosimetry ROSED in a clinical setting by utilizing knowledge acquired preclinically. Patients with pathologically confirmed epithelioid malignant pleural mesothelioma were enrolled in a phase II randomized clinical trial of extended pleurectomy/decortication with or without Photofrin-mediated PDT. Photofrin (provided by Pinnacle Biologics, Chicago, IL, USA) was administered at 2 mg per kg of body weight as an intravenous infusion approximately 24 h prior to the anticipated time of intraoperative PDT. After surgically resecting all gross disease, PDT treatment was performed with 630 nm light to a total fluence of 60 J cm⁻² as previously described (30–34). Briefly, the pleural cavity was filled with diluted Intralipid solution to aid with light scattering and 60 J cm⁻² 630 nm light was delivered to the pleural cavity via an optical fiber inserted into modified endotracheal tube filled with 0.1% Intralipid. Homogeneous light delivery is accomplished by continuously moving the light source around the pleural cavity with continuous feedback monitoring of light fluence rate and cumulative fluence provided by 8 isotropic detectors (Medlight, Switzerland) sutured to the chest wall. Four of the eight isotropic detectors were used to monitor the light dose and Photofrin fluorescence simultaneously. Long pass filters (Semrock, Inc., Rochester, NY, USA) were used to block the treatment light before the fluorescence was recorded by 4 single-channel spectrometers (Exemplar, B&W Tek, Inc., Newark, DE, USA).

A schematic diagram of ROSED dosimeter which consists of a PDT dose dosimeter and a DCS module is shown in Fig. 1(a). PDT dose dosimeter consists of photodiodes for light fluence rates measurements and spectrometers for fluorescence measurements. More details about PDT dosimeter and the quantification of absolute Photofrin concentration from measured fluorescence spectra can be found in (19).

Measurement of blood flow during clinical PDT. DCS monitoring of tissue blood flow during pleural PDT was implemented using a custom-built DCS contact probe as shown in Fig. 1(b). The contact probe consists of a side-firing multimode source fiber and three single-mode

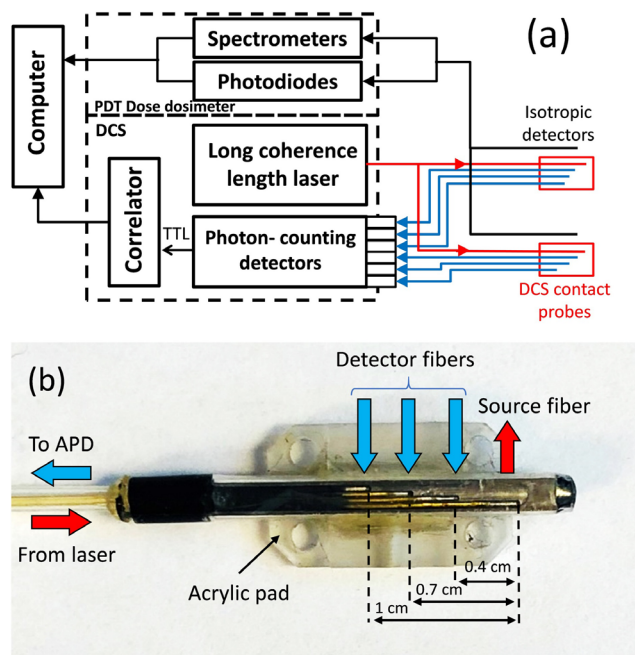


Figure 1. (a) Schematic diagram of the PDT dosimeter and DCS, (b) a picture of the DCS contact probe, which consists of one multimode source fiber and 3 single-mode detector fibers positioned at 0.4, 0.7 and 1 cm laterally from the source.

detector fibers polished at 45°. Light from a continuous wave 785 nm laser with long coherence length was delivered through the source fiber. The reflected diffuse light was collected using the detector fibers located at 0.4, 0.7 and 1.0 cm from the source fiber, which correspond to a range of probed tissue depth between 0.2 to 0.5 cm. Three single photon counting avalanche photodiodes were used to detect the diffuse light in parallel. The DCS probe was mounted onto a clear acrylic rectangle pad with small holes at each corner that allowed it to be sutured adjacent to one of the isotropic detectors measuring light fluence rate and photosensitizer fluorescence data. Tissue blood flow was measured continuously throughout the PDT treatment. The study started with one DCS contact probe for the first two patients, and it was later expanded for the next five patients to include the second DCS contact probe to enable simultaneous measurements of blood flow at two different pleural sites.

Calculation of [ROS]rx using ROSED. The PDT process is described by a set of kinetic equations which can be simplified to compute the production of [ROS]rx (4,8,9,13). These equations are dependent on the temporal and spatial distribution of light fluence rate (ϕ), photosensitizer concentration ($[S_0]$), ground state oxygen concentration ($[^3O_2]$), oxygen supply rate (g) and the photosensitizer-specific reaction-rate parameters (δ , β , σ and ξ). The relevant equations are:

$$\frac{d[S_0]}{dt} = -\frac{[^3O_2]}{[^3O_2] + \beta} ([S_0] + \delta) \phi [S_0] \xi \sigma, \quad (1)$$

$$\frac{d[^3O_2]}{dt} = -\frac{[^3O_2]}{[^3O_2] + \beta} \phi [S_0] \xi + g \left(1 - \frac{[^3O_2]}{[^3O_2]_0} \right), \quad (2)$$

$$\frac{d[ROS]_{rx}}{dt} = \xi \frac{[^3O_2]}{[^3O_2] + \beta} \phi [S_0]. \quad (3)$$

Definitions and values of the five specific PDT photochemical parameters for Photofrin are given in Table 1. Since light fluence rate, Photofrin concentration and tissue oxygen were measured in this study, only Eq. (3) is needed to calculate for [ROS]rx. For the calculation of [ROS]rx, the term on the right-hand side of Eq. (3) is integrated over the time course of PDT treatment using the measured value of $[^3O_2]$, $[S_0]$ and light fluence rate. In vivo light fluence rate distribution can be

estimated from the in-air light fluence rate using a 6-parameter analytic expression (35). Tissue optical properties needed for this calculation were obtained from diffuse reflectance measurements using the multifiber contact probe. Besides using the value of $[^3O_2]$ measured by Oxylite Pro, we also investigated the use of tissue blood flow measured by DCS during PDT to calculate for [ROS]rx. The rationale of using tissue blood flow as a surrogate for $[^3O_2]$ is because convective supply of oxygen depends directly on blood flow. Changes in tissue oxygenation depend critically on oxygen consumption and supply by blood flow. A conversion factor of $1.5 \times 10^9 \mu\text{Ms cm}^{-2}$ was found to be needed to scale the blood flow index to match the measured tissue oxygen. [ROS]rx calculated based on $[^3O_2]$ measured by Oxylite was compared with that determined based on DCS blood-flow-derived oxygen.

RESULTS

Chlorophyll spectra in mouse fluorescence measurements

Figure 2(a) shows the spectral comparison of mouse tissue auto-fluorescence, chlorophyll fluorescence and Photofrin fluorescence. Chlorophyll fluorescence spectrum has a peak at ~675 nm, which overlaps significantly with the fluorescence spectrum of Photofrin. This chlorophyll peak could significantly contaminate the measured fluorescence and complicate the calculation of Photofrin concentrations. Our data suggest that chlorophyll signal decayed quickly after the mice were fed with the modified diet and its peak intensity reduced to <5% of the initial value, 10 days after diet change (Figure 2(b)). All Photofrin measurements in this study were taken at least two weeks after the mice were fed with chlorophyll-free rodent diet to make sure fluorescence measurements were not affected by the presence of chlorophyll.

Correlation between tumor oxygen and blood flow

Figure 3 shows the comparison of tissue oxygen measured using two different techniques for seven mice during PDT treatment: blue lines for Oxylite Pro measurements and red lines for DCS measurements. For Oxylite Pro measurements, tumor oxygen (in μM) was approximated from the measured tumor oxygen tension (in mmHg) by multiplying by $1.295 \mu\text{M mmHg}^{-1}$. For DCS measurements, tumor oxygen was approximated from the blood flow index ($\text{cm}^2 \text{s}^{-1}$) using the conversion factor of $1.5 \times 10^9 \mu\text{Ms cm}^{-2}$. We have previously demonstrated (8,36), in murine models, that the magnitude of DCS-measured blood flow index can be scaled by a factor of 1.5×10^9 to match the magnitude of the tumor oxygen level at the beginning of light delivery for PDT. Indeed, in the present investigation, we computed the average ratio of the entire spectrum of tumor oxygen

Table 1. Model parameters used in the macroscopic kinetics equations for Photofrin.

Parameter	Definition	Value	References
ϵ ($\text{cm}^{-1} \mu\text{M}^{-1}$)	Photofrin extinction coefficient	3.5×10^{-3} (4)	
ξ ($\text{cm}^2 \text{s}^{-1} \text{mW}^{-1}$)	Specific oxygen consumption rate	3.7×10^{-3} (4)	
σ (μM^{-1})	Specific photobleaching ratio	7.6×10^{-5} (4)	
β (μM)	Oxygen quenching threshold concentration	11.9 (4)	
δ (μM)	Low-concentration correction	33 (4)	

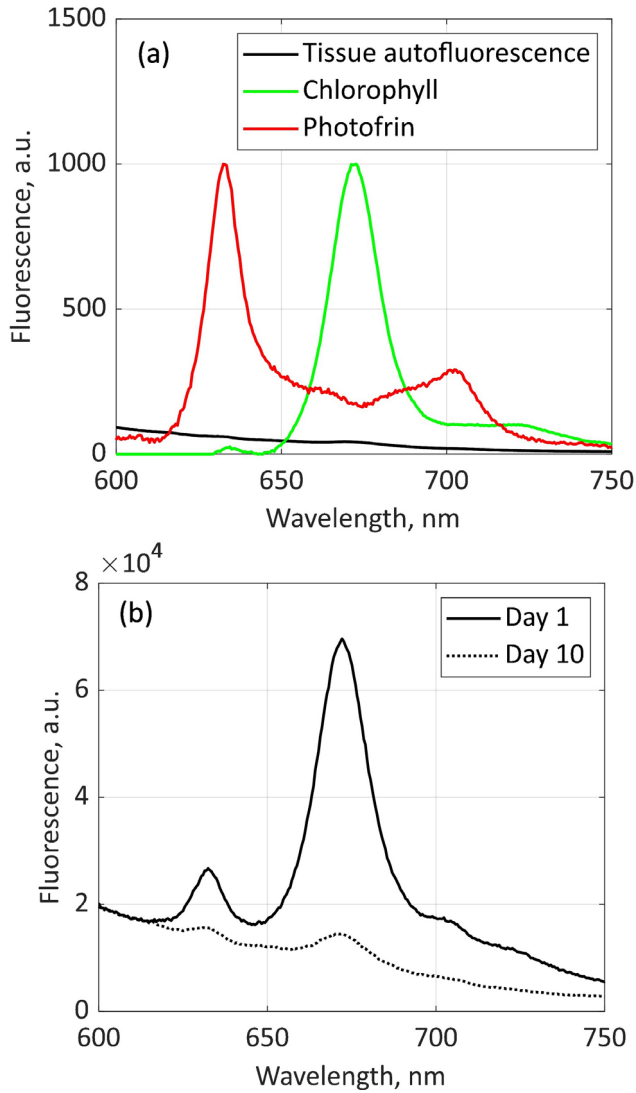


Figure 2. (a) Spectra of mouse tissue autofluorescence, chlorophyll fluorescence and Photofrin fluorescence; (b) Fluorescence spectra taken from mice a day (solid line) and 10 days (dotted line) after feeding on chlorophyll-free rodent diet. Fluorescence peak intensity at 675nm on day 10 was less than 5% of the initial peak intensity on day 1.

to tumor blood flow for all mice investigated and determined a similar blood flow index to tumor oxygen conversion factor of $\sim 1.5 \times 10^9 \mu\text{Ms cm}^{-2}$. Generally, results in Fig. 3 show large variation in temporal changes of tumor oxygenation for mice treated with similar and different PDT treatment conditions. Measurements of tumor oxygen during PDT is therefore very important for accurate ROSED, since the heterogeneities in temporal changes in tumor oxygen cannot be modeled using Eq. 2.

Although the overall trends in tumor oxygen obtained from OxyLite and DCS measurements are in good agreement, there are subtle differences in the absolute level of oxygen concentration between the two methods. To test if these differences would affect the accuracy of ROSED, we calculated and compared the cumulative [ROS]rx using Eq. 3 based on OxyLite-measured [$^3\text{O}_2$] and blood-flow-derived [$^3\text{O}_2$]. A summary of the treatment conditions for the seven mice, including in-air light fluence rate, treatment time, initial Photofrin concentration in tumors [S_0] and the calculated total reacted reactive oxygen species concentration

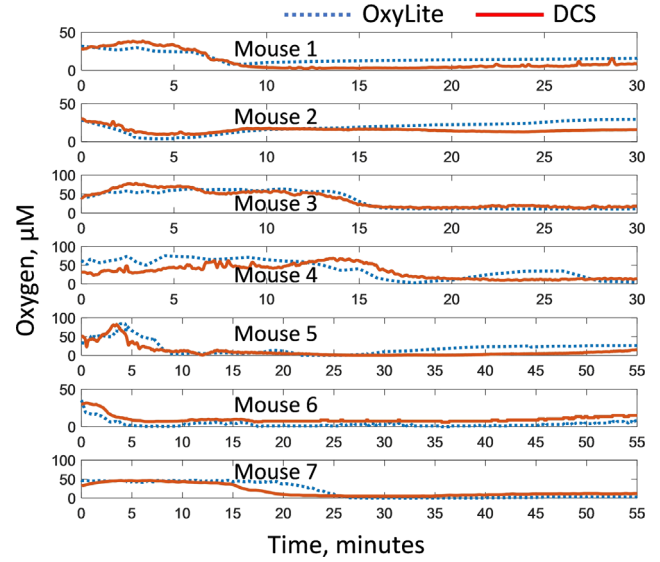


Figure 3. Comparison of tissue oxygen measured using the OxyLite Pro (blue dotted lines) and blood-flow-derived tissue oxygen estimated as the product of the blood flow index and a conversion factor of $1.5 \times 10^9 \mu\text{Ms cm}^{-2}$ (red solid lines).

[ROS]rx are given in Table 2. It should be noted that Photofrin concentrations were measured at different timepoints during PDT treatment to account for photobleaching, but only initial values of Photofrin concentration are reported here. Despite differences in the absolute level of tumor oxygen, the calculated [ROS]rx based on the two oxygen measurement methods are in close agreement as shown in Table 2. Differences between the calculated [ROS]rx based on OxyLite-measured [$^3\text{O}_2$] and blood-flow-derived [$^3\text{O}_2$] data are within 12% for all mice. This suggests that tumor blood flow index, which can be measured noninvasively during clinical PDT, can legitimately be used to derive tumor oxygenation and to calculate for [ROS]rx with desired accuracy. It should be noted that all seven mice used in this study were a subset of the animals used in a previous report (9), in which a more comprehensive investigation on the correlation between [ROS]rx and treatment outcomes can be found.

Temporal and spatial distribution of light fluence rate, oxygen and Photofrin during pleural PDT

Figure 4 shows explicit measurements of light fluence rate, blood-flow-derived oxygen and Photofrin concentration at two different sites in the pleural cavities of two patients (Figs 4(a), (c) and (e) are for patient #37, and Figs 4(b), (d) and (f) are for patient #38) during PDT treatment. Figure 4(a) shows temporal changes in light fluence rate detected on the tissue surface of apex (blue line) and posterior mediastinum (red line) in the pleural cavity of patient #37 during the time course of PDT treatment; and Fig. 4(b) shows the treatment light fluence rate detected on the tissue surface of posterior mediastinum (blue line) and posterior sulcus (red line) for patient #38. Rapid and large fluctuations in the detected light fluence rates were observed for all pleural sites and for all patients (not shown in Fig. 4). These fluctuations in treatment light fluence rate are due to movement of the treatment light wand in the pleural cavity as the PDT surgeon “paints” the light dose uniformly over the entire pleural cavity. High fluence rates (up to 600 mW cm^{-2})

Table 2. In-air light fluence rate (ϕ_{air}), treatment time, initial Photofrin concentration in tumors [PS] and total reacted reactive oxygen species concentration [ROS]_{rx} calculated based on measured [³O₂] and DCS blood flow.

Index	Mouse #	In-air light fluence rate, ϕ_{air} (mW cm ⁻²)	Treatment time (s)	Initial Photofrin concentration, [PS] (μM)	Calculated [ROS] _{rx} (mM)	
					Measured [³ O ₂]	DCS blood flow
1	12-1	75	1800	6.9	1.39	1.35
2	12-2	75	1800	6.8	1.24	1.18
3	12-3	75	1800	5.2	1.07	1.12
4	12-4	75	1800	5.7	1.09	0.95
5	11-2	75	3333	6.5	2.33	2.21
6	11-3	75	3333	4.2	1.73	1.92
7	11-4	75	3333	4.5	1.89	1.81

were detected when the PDT treatment wand was in close proximity to an isotropic detector. Very low or no treatment light fluence rate was detected when the PDT treatment wand was moved away from an isotropic detector to a distant pleural site. Light fluence dosimetry at pleural sites, where no DCS measurement was performed, are not reported in this paper.

Figures 4(c) and (d) show the temporal changes in tumor oxygen measured at the same pleural sites (as in (a) and (b)) for patient #37 and patient #38. Oxygen concentrations were approximated from the blood flow index obtained from DCS measurements, by multiplying the DCS blood flow index by the conversion factor determined preclinically (as described above).

We can see that tumor oxygen levels were low at the beginning of PDT treatment, suggesting tissue hypoxia due to surgical damage of the tissue vasculature. As PDT starts, tumor oxygen fluctuates significantly, and the fluctuation patterns are distinct from site-to-site and from patient-to-patient during light delivery. Interestingly, fluctuations in tumor oxygen were correlated with variations in light fluence rate. Figures 4(g) and (h) show overlay plots of fluence rate and tumor oxygen taken from apex and PM locations in patient #37. Comparison between light fluence rate and tumor oxygen shows that high fluence rate induces rapid increase in tumor blood flow and hence increase in tumor oxygen. During periods of low light fluence rate, tissue blood flow (oxygen) decreases and/or returns to the baseline level.

Figures 4(e) and (f) plots temporal changes in local Photofrin concentration measured at two pleural sites for patient #37 and patient #38. Only Photofrin concentration at sites where DCS measurement was performed are shown. Each data point in Fig. 4(e) and (f) represents a Photofrin concentration that is obtained from one fluorescence spectrum using the method described elsewhere (19). Photofrin concentrations are corrected for variation in tissue optical properties, obtained using diffuse reflectance spectroscopy, based on an analytical correction function (19). Photofrin fluorescence was excited using the PDT treatment laser. The highly fluctuating treatment light fluence rate, due to the fact that the light source was constantly circulating in the lung cavity, resulted in $\pm 15\%$ uncertainty in the extracted Photofrin concentration. Mean concentration of Photofrin was calculated for all data points every 10 min of treatment time, and the results are shown as solid lines in each plot. The mean Photofrin concentrations exhibit no sign of photobleaching for all measurement sites and for all patients (including data not shown) during the time course of PDT treatment. The mean Photofrin concentrations for each pleural site was used for the

calculation of [ROS]_{rx} using ROSED and are summarized in Table 3.

Calculated [ROS]_{rx} using ROSED for clinical PDT

Cumulative [ROS]_{rx} generated by PDT was calculated using ROSED by integrating the right-hand side of Eq. 3 over the time course of PDT treatment. Temporal and spatial distribution of light fluence rate on the tissue surface (ϕ), mean Photofrin concentration ($[S_0]$), blood-flow-derived tumor oxygen ($[^3\text{O}_2]$) and photophysical parameters (ξ and β) are needed for the calculation of [ROS]_{rx}. The ROSED-calculated [ROS]_{rx} (mM) for 12 sites in seven patients are summarized in Table 3. Comparison to other commonly used dose metrics, namely light fluence (J cm^{-2}), and the PDT dose ($\mu\text{M J cm}^{-2}$) defined as the product of light fluence and photosensitizer concentration, are also included in Table 3. Tissue optical properties used for the correction of Photofrin concentration, and the resultant mean corrected Photofrin concentration ($[\text{Photofrin}]$) are also provided. The mean (standard deviation) optical properties (μ_a, μ_s') of all pleural tissues for the seven patients are 0.37 ± 0.15 and $9.4 \pm 2.2 \text{ cm}^{-1}$, respectively. The mean Photofrin concentration of all pleural tissues for seven patients is $6.2 \pm 2.1 \text{ mg kg}^{-1}$. Note, 1 mg kg^{-1} of Photofrin is equivalent to $1.65 \mu\text{M}$ of Photofrin. PDT treatments were delivered based on light dosimetry until the prescribed 60 J cm^{-2} of light fluence. Therefore, the light fluence detected at the surface for all pleural sites are equal as shown in Table 3.

Despite using the same light dose, PDT dose delivered to all sites can be quite different. The mean (standard deviation) PDT dose delivered to these seven patients is $614 \pm 202.6 \mu\text{M J cm}^{-2}$, with a maximum of $1029.6 \mu\text{M J cm}^{-2}$ and minimum of $382.1 \mu\text{M J cm}^{-2}$. The variations in delivered PDT dose are mainly due to the intra- and interpatient heterogeneities in Photofrin uptake. Lastly, assessment of ROSED reveals large variation in the calculated [ROS]_{rx} for all patients, with a mean (standard deviation) of $0.59 \pm 0.25 \text{ mM}$ and a range of $0.31\text{--}1.17 \text{ mM}$. These values are consistent with those reported in previous preclinical Photofrin-mediated PDT studies (4,8,9,37).

DISCUSSION

Treatment light fluence is the most commonly used dose metric for clinical PDT dosimetry due to its simplicity of measurement and correlation to treatment outcome. PDT dose is a better metric

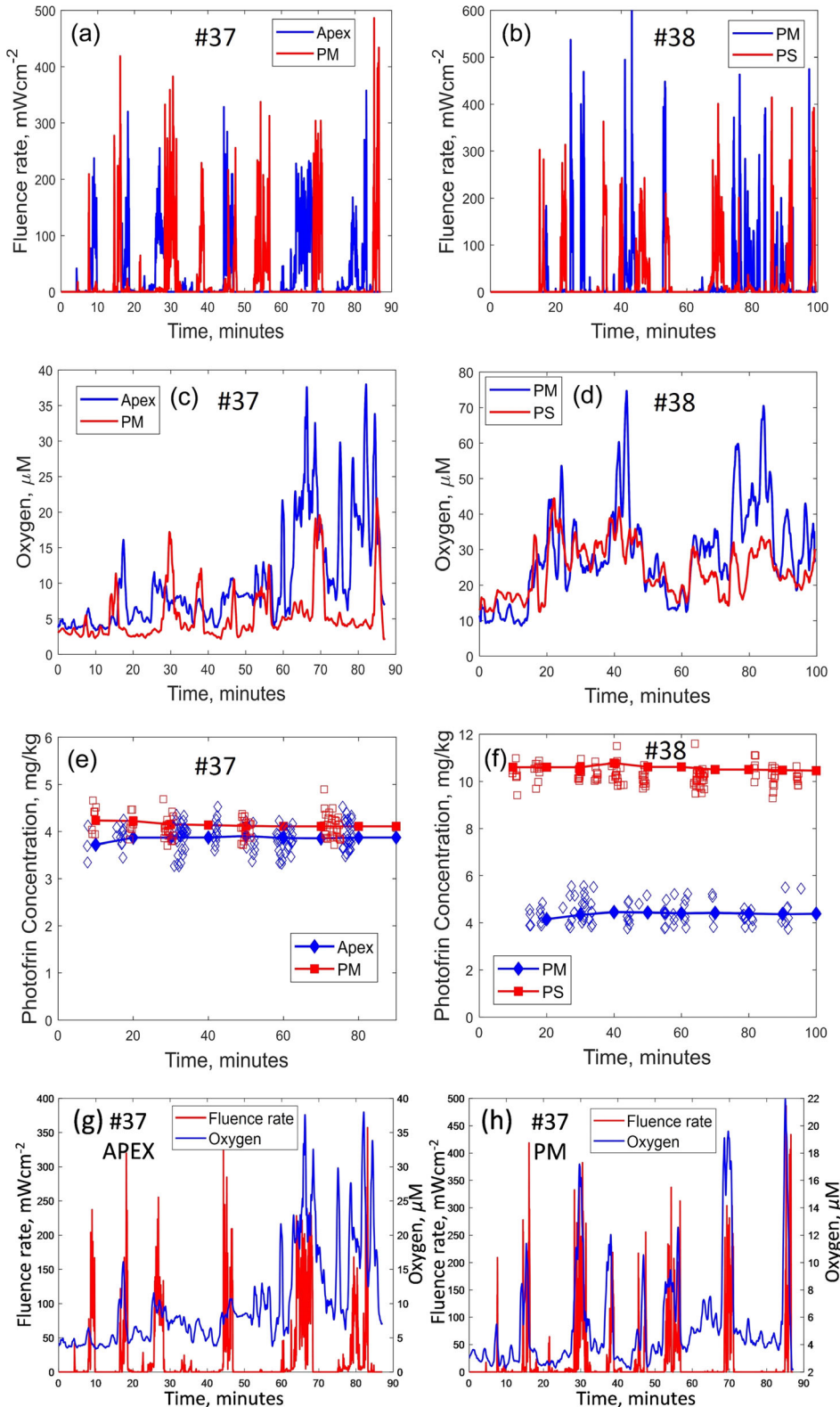


Figure 4. Real-time measurements of (a–b) treatment fluence rate, (c–d) blood-flow-derived oxygen and (e–f) Photofrin concentration measured from two pleural cavity sites. (a), (c) and (e) are measurements taken from patient #37; (b), (d) and (f) are measurements taken from patient #38. (g) and (h) are overlay plots of fluence rate and oxygen measurements taken from patient #37.

than light fluence alone, with improved treatment outcome prediction because it accounts for variations in tumor photosensitizer uptake. Our group has demonstrated the feasibility of clinical

PDT dose dosimetry by concurrent measurement of light fluence rate and photosensitizer concentration during PDT. In preclinical investigations, $[ROS]_{rx}$ or $[^1O_2]_{rx}$ for type-II PDT only, have

Table 3. Tissue optical properties, mean Photofrin concentration, light fluence, PDT dose and [ROS]rx at the surface of 12 pleural sites on seven patients. The light fluence rate on surface is the same at 60 J cm⁻² for all patients.

Patient	Site	μ_a (cm ⁻¹)	μ_s' (cm ⁻¹)	[Photofrin] (mg kg ⁻¹)	Light fluence at surface (J cm ⁻²)	PDT dose (μ M J cm ⁻²)	[ROS]rx (mM)
#20	PM	0.42	10.3	7.2	60	710.8	0.69
#27	ACW	0.32	8.9	5.7	60	564.3	0.34
#29	PCW	0.65	13.2	9.8	60	965.3	1.17
	ACW	0.38	9.6	6.0	60	594.0	0.46
#35	PM	0.48	9.2	5.7	60	564.3	0.85
	AS	0.35	9.1	6.7	60	663.3	0.33
#37	PM	0.17	5.9	4.1	60	396.0	0.75
	Apex	0.22	6.3	3.9	60	382.1	0.59
#38	PM	0.23	6.8	4.4	60	435.6	0.41
	PS	0.62	12.3	10.4	60	1029.6	0.72
#40	PM	0.25	10.2	4.1	60	403.9	0.31
	AS	0.35	11.2	6.7	60	659.3	0.41
Average		0.37 \pm 0.15	9.4 \pm 2.2	6.2 \pm 2.1	60	614 \pm 202.6	0.59 \pm 0.25

ACW = anterior chest wall; AS = anterior sulcus; PCW = posterior chest wall; PM = posterior mediastinum; PS = posterior sulcus. 1 mg kg⁻¹ Photofrin = 1.65 μ M Photofrin.

been demonstrated to be the best dose metric to predict PDT treatment outcome (4–6); however, its clinical implementation is challenging due to a lack of FDA-approved instrument to measure tissue oxygenation reliably during PDT.

For our work, we employ the ROSED model (Eq. 2). In principle, it can be used to estimate [³O₂] when PS-specific photo-physical parameters are known, and the estimated [³O₂] is found to be in close agreement with measured tumor oxygen during preclinical PDT using several photosensitizers, including HPPH and BPD (10,11). However, for Photofrin-mediated PDT, large mouse-to-mouse heterogeneity in tumor oxygen changes has been observed in preclinical studies (8,27) and these intersubject variations in [³O₂] cannot be modeled using Eq. (2). Thus, explicit measurement of tumor oxygen is needed to improve the accuracy of the calculated [ROS]rx to better predict for treatment outcome.

Since the convective oxygen delivery depends directly on blood flow, increasing blood flow will increase the delivery of oxygen via the blood to the tissues. Our previous simulation study (20) showed that maximum oxygen supply rate (g) increases linearly with blood flow velocity (v_2). Indeed, in our present investigation, we observed that changes in tumor blood flow during PDT correlates well with the temporal changes in tumor oxygen (see Fig. 3). Tumor blood flow is measured using DCS, which is a noninvasive optical modality that can be employed clinically to collect patient's blood flow data. The average ratio of tumor oxygen to tumor blood flow for all mice was determined to be 1.5×10^9 . The conversion factor has a unit of μ M s cm⁻²; hence the blood-flow-derived tumor oxygen (blood flow index multiplied by conversion factor) has the same units as measured tumor oxygen (μ M). Although a single 1.5×10^9 conversion factor between these two parameters was used in this study, we have observed variations in the conversion factor between mice, between 1×10^9 to 2×10^9 in previous reports (8,10,27,36). Mouse-to-mouse variation and temporal change in the conversion factor could happen over the course of a treatment and contribute to the subtle mismatches between OxyLite-measured tumor oxygen and blood-flow-derived tumor oxygen traces as shown in Fig. 3. However, we found that the variation in the conversion factor (between 1×10^9 to 2×10^9) has impacted minimally on the value of calculated [ROS]rx based on blood-flow-derived oxygen.

Tissue optical properties used to determine blood flow indices were obtained from diffuse reflectance measured before the beginning of PDT treatment. Tissue optical properties were assumed to be constant during the time course of PDT. Irwin et al. (38) has investigated the effect of optical properties on the DCS blood flow indices and found that μ_s' has a greater influence on blood flow than μ_a . However, one should expect larger temporal variation in tissue μ_a than μ_s' , due to the rapid and large fluctuations in tumor blood flow that would cause the total hemoglobin concentration to change significantly. μ_s' depends on the size, morphology and structure of the tissue components and is less likely to highly vary during the time course of a PDT treatment. Based on Irwin's investigation, a 150% change in tissue absorption would result in approximately 40% error in the estimated blood flow index. Therefore, small mismatches between traces of OxyLite-measured tumor oxygen and blood-flow-derived tumor oxygen as shown in Fig. 3 could be due to over- or underestimation of blood flow indices caused by false assumption of constant tissue optical properties in this study. For future PDT studies, concurrent measurements of DCS and optical properties would be useful to account for temporal variations in tissue μ_a and μ_s' . Nevertheless, despite the potential error in blood-flow-derived tumor oxygen as discussed above, [ROS]rx calculated based on blood flow in this study are in very good agreement with the [ROS]rx calculated using measured [³O₂]. We found that small differences in [³O₂] have minimal impact on the calculation of [ROS]rx.

In conclusion, for the first time, we performed ROSED in a clinical setting with concurrent explicit measurements of light fluence rate and PS concentration using a PDT dose dosimeter, and blood flow using DCS. Tumor oxygenation was estimated by multiplying DCS blood flow index by a preclinically determined conversion factor of 1.5×10^9 μ M s cm⁻². The mean (standard deviation) of calculated [ROS]rx from a total of 12 pleural sites and seven patients is 0.59 ± 0.25 mM. The results reveal large inter- and intrapatient heterogeneity in [ROS]rx, although PDT treatment was performed to a prescribed light dose of 60 J cm⁻². ROSED has been demonstrated in preclinical studies to be a useful predictor of treatment outcome, because it accounts for both subject-to-subject and site-to-site variations in PS concentration and tissue oxygenation. As for clinical studies, due to ongoing status of clinical trial, treatment outcome

information is still blinded and not assessable for the subjects who were recruited in this manuscript. A more detailed investigation of correlation between model-calculated [ROS]rx with clinical outcomes will be performed when data become available in the near future. Nevertheless, this study suggests that real-time ROSED could be explored to guide physicians in creating a homogenous [ROS]rx at all areas of disease, thereby providing for the desired treatment goal.

Acknowledgements—The authors would like to thank all the PDT group members at the hospital of the University of Pennsylvania, Carmen Rodriguez, Rozhin Penjweini, Arash Darafsheh, Charles B Simone II, Jess Appleton, Sally McNulty, Joann Miller, and Min Yuan. This work was supported by NIH grants R01 NS060653, R01 CA154562, R01 CA236362, P41 EB015893 and P01 CA87971 and by the Department of Radiation Oncology.

REFERENCES

- Dougherty, T. J., C. J. Gomer, B. W. Henderson, G. Jori, D. Kessel, M. Korbelik, J. Moan and Q. Peng (1998) Photodynamic therapy. *J Natl Cancer Inst* **90**, 889–905.
- Agostinis, P., K. Berg, K. A. Cengel, T. H. Foster, A. W. Girotti, S. O. Gollnick, S. M. Hahn, M. R. Hamblin, A. Juzeniene, D. Kessel, M. Korbelik, J. Moan, P. Mroz, D. Nowis, J. Piette, B. C. Wilson and J. Golab (2011) Photodynamic therapy of cancer: An update. *Cancer J. Clin.* **61**(4), 250–281.
- Allison, R. R. and K. Moghissi (2013) Photodynamic therapy (PDT): PDT mechanisms. *Clin. Endosc.* **46**, 24–29.
- Qiu, H., M. M. Kim, R. Penjweini and T. C. Zhu (2016) Macroscopic singlet oxygen modeling for dosimetry of Photofrin-mediated photodynamic therapy: an in-vivo study. *J. Biomed. Opt.* **21**, 88002–88002.
- Penjweini, R., M. M. Kim, B. Liu and T. C. Zhu (2016) Evaluation of the 2-(1-Hexyloxyethyl)-2-devinyl pyropheophorbide (HPPH) mediated photodynamic therapy by macroscopic singlet oxygen modeling. *J. Biophotonics* **9**, 1344–1354.
- Kim, M. M., R. Penjweini and T. C. Zhu (2017) Evaluation of singlet oxygen explicit dosimetry for predicting treatment outcomes of benzoporphyrin derivative monoacid ring A-mediated photodynamic therapy. *J Biomed Opt* **22**, 1–10.
- Yamamoto, J., S. Yamamoto, T. Hirano, S. Li, M. Koide, E. Kohno, M. Okada, C. Inenaga, T. Tokuyama, N. Yokota, S. Terakawa and H. Namba (2006) Monitoring of singlet oxygen is useful for predicting the photodynamic effects in the treatment for experimental glioma. *Clin. Cancer Res.* **12**, 7132–7139.
- Penjweini, R., M. M. Kim, Y. H. Ong and T. C. Zhu (2017) Singlet oxygen explicit dosimetry to predict long-term local tumor control for Photofrin-mediated photodynamic therapy. Proc. SPIE 1004711.
- Sheng, T., Y. H. Ong, T. M. Busch and T. C. Zhu (2019) Reactive oxygen species explicit dosimetry to predict local tumor control for Photofrin-mediated photodynamic therapy. Proc. SPIE 108600V.
- Penjweini, R., M. M. Kim, Y. H. Ong and T. C. Zhu (2017) Singlet oxygen explicit dosimetry to predict local tumor control for HPPH-mediated photodynamic therapy. Proc. SPIE 1004710.
- Kim, M. M., R. Penjweini, Y. H. Ong and T. C. Zhu (2017) Singlet oxygen explicit dosimetry to predict long-term local tumor control for BPD-mediated photodynamic therapy. Proc. SPIE 100470X.
- Wei, Y., J. Zhou, D. Xing and Q. Chen (2007) In vivo monitoring of singlet oxygen using delayed chemiluminescence during photodynamic therapy. *J. Biomed. Opt.* **12**(1–7), 7.
- Ong, Y. H., M. M. Kim and T. C. Zhu (2018) Photodynamic therapy explicit dosimetry. In *Recent Advancements and Applications in Dosimetry*, Vol. 1, (Edited by M. F. Chan) pp. 45–72. Nova Science Publishers, Inc, Hauppauge, NY.
- Jarvi, M. T., M. S. Patterson and B. C. Wilson (2012) Insights into photodynamic therapy dosimetry: simultaneous singlet oxygen luminescence and photosensitizer photobleaching measurements. *Biophys. J.* **102**, 661–671.
- Jarvi, M. T., M. J. Niedre, M. S. Patterson and B. C. Wilson (2006) Singlet oxygen luminescence dosimetry (SOLD) for photodynamic therapy: current status, challenges and future prospects. *Photochem. Photobiol.* **82**, 1198–1210.
- Wang, K. K.-H., J. C. Finlay, T. M. Busch, S. M. Hahn and T. C. Zhu (2010) Explicit dosimetry for photodynamic therapy: macroscopic singlet oxygen modeling. *J. Biophotonics* **3**, 304–318.
- Zhu, T. C., J. C. Finlay, X. Zhou and J. Li (2007) Macroscopic modeling of the singlet oxygen production during PDT. Proc. SPIE 642708.
- Finlay, J. C., T. C. Zhu, A. Dimofte, J. S. Friedberg and S. M. Hahn (2006) Diffuse reflectance spectra measured in vivo in human tissues during Photofrin-mediated pleural photodynamic therapy. Proc. SPIE 613900.
- Ong, Y. H., M. M. Kim, J. C. Finlay, A. Dimofte, S. Singhal, E. Glatstein, K. A. Cengel and T. C. Zhu (2017) PDT dose dosimetry for Photofrin-mediated pleural photodynamic therapy (pPDT). *Phys. Med. Biol.* **63**, 015031.
- Zhu, T. C., B. Liu and R. Penjweini (2015) Study of tissue oxygen supply rate in a macroscopic photodynamic therapy singlet oxygen model. *J. Biomed. Opt.* **20**, 038001–038001.
- Whiteley, J. P., D. J. Gavaghan and C. E. Hahn (2002) Mathematical modelling of oxygen transport to tissue. *J. Math. Biol.* **44**, 503–522.
- Yu, G., T. Durduran, C. Zhou, H. W. Wang, M. E. Putt, H. M. Saunders, C. M. Sehgal, E. Glatstein, A. G. Yodh and T. M. Busch (2005) Noninvasive monitoring of murine tumor blood flow during and after photodynamic therapy provides early assessment of therapeutic efficacy. *Clin. Cancer Res.* **11**, 3543–3552.
- Lemieux, P. A. and D. J. Durian (1999) Investigating non-Gaussian scattering processes by using nth-order intensity correlation functions. *J. Opt. Soc. Am. A* **16**, 1651–1664.
- Boas, D. A. and A. G. Yodh (1997) Spatially varying dynamical properties of turbid media probed with diffusing temporal light correlation. *J. Opt. Soc. Am. A* **14**, 192–215.
- Boas, D. A., L. E. Campbell and A. G. Yodh (1995) Scattering and imaging with diffusing temporal field correlations. *Phys. Rev. Lett.* **75**, 1855–1858.
- Baker, W. B., A. B. Parthasarathy, D. R. Busch, R. C. Mesquita, J. H. Greenberg and A. G. Yodh (2014) Modified Beer-Lambert law for blood flow. *Biomed. Opt. Express* **5**, 4053–4075.
- Ong, Y. H., M. M. Kim, R. Penjweini, C. E. Rodriguez, A. Dimofte, J. C. Finlay, T. M. Busch, A. G. Yodh, K. A. Cengel, and T. C. Zhu (2017) Monitoring and assessment of tumor hemodynamics during pleural PDT. Proc. SPIE 100470C.
- Delpy, D. T., M. Cope, P. van der Zee, S. Arridge, S. Wray and J. Wyatt (1988) Estimation of optical pathlength through tissue from direct time of flight measurement. *Phys. Med. Biol.* **33**, 1433–1442.
- Farzam, P., E. M. Buckley, P.-Y. Lin, K. Hagan, P. E. Grant, T. E. Inder, S. A. Carp and M. A. Franceschini (2017) Shedding light on the neonatal brain: probing cerebral hemodynamics by diffuse optical spectroscopic methods. *Sci. Rep.* **7**, 15786.
- Friedberg, J. S., C. B. 2nd Simone, M. J. Culligan, A. R. Barsky, A. Doucette, S. McNulty, S. M. Hahn, E. Alley, D. H. Serman, E. Glatstein and K. A. Cengel (2017) Extended pleurectomy-decortication-based treatment for advanced stage epithelial mesothelioma yielding a median survival of nearly three years. *Ann. Thoracic Surg.* **103**, 912–919.
- Friedberg, J. S., M. J. Culligan, R. Mick, J. Stevenson, S. M. Hahn, D. Serman, S. Punekar, E. Glatstein and K. Cengel (2012) Radical pleurectomy and intraoperative photodynamic therapy for malignant pleural mesothelioma. *Ann. Thoracic Surg.* **93**, 1658–1665.
- Friedberg, J. S., R. Mick, M. Culligan, J. Stevenson, A. Fernandes, D. Smith, E. Glatstein, S. M. Hahn and K. Cengel (2011) Photodynamic therapy and the evolution of a lung-sparing surgical treatment for mesothelioma. *Ann. Thoracic Surg.* **91**, 1738–1745.
- Du, K. L., S. Both, J. S. Friedberg, R. Rengan, S. M. Hahn and K. A. Cengel (2010) Extrapleural pneumonectomy, photodynamic therapy and intensity modulated radiation therapy for the treatment of malignant pleural mesothelioma. *Cancer Biol. Ther.* **10**, 425–429.
- Simone, C. B. 2nd and K. A. Cengel (2014) Photodynamic therapy for lung cancer and malignant pleural mesothelioma. *Semin. Oncol.* **41**, 820–830.

35. Ong, Y. H. and T. C. Zhu (2016) Analytic function for predicting light fluence rate of circular fields on a semi-infinite turbid medium. *Opt. Express* **24**, 26261–26281.
36. Ong, Y. H., M. M. Kim, Z. Huang and T. C. Zhu (2018) Reactive oxygen species explicit dosimetry (ROSED) of a type 1 photosensitizer. Proc. SPIE 104760V.
37. Qiu, H., M. M. Kim, R. Penjweini, J. C. Finlay, T. M. Busch, T. Wang, W. Guo, K. A. Cengel, C. B. II Simone, E. Glatstein and T. C. Zhu (2017) A comparison of dose metrics to predict local tumor control for photofrin-mediated photodynamic therapy. *Photochem. Photobiol.* **93**, 1115–1122.
38. Irwin, D., L. Dong, Y. Shang, R. Cheng, M. Kudrimoti, S. D. Stevens and G. Yu (2011) Influences of tissue absorption and scattering on diffuse correlation spectroscopy blood flow measurements. *Biomed. Opt. Express* **2**, 1969–1985.